Aberrant methylation and expression of TNXB promotes chondrocyte apoptosis and extracullar matrix degradation in hemophilic arthropathy via AKT signaling

Jiali Chen [1, 2, †], Zeng Qinghe [1, 2, †], Xu Wang [1, 2], Rui Xu [3], Weidong Wang [4], Yuliang Huang [4], Qi Sun [5], Wenhua Yuan [1], Pinger Wang [1], Di Chen[6, 7 *], Peijian Tong [8 *], Hongting Jin [1, *]

[1] Institute of Orthopaedics and Traumatology, the First Affiliated Hospital of Zhejiang Chinese Medical University，Zhejiang Provincial Hospital of Chinese Medicine, Hangzhou, Zhejiang, China

[2] The First College of Clinical Medicine, Zhejiang Chinese Medical University, Hangzhou, China

[3] Department of Orthopedics, Affiliated Hospital of Jiangxi University of Traditional Chinese Medicine, Nanchang, Jiangxi, China.

[4] Department of Osteology, The Second Affiliated Hospital of Zhejiang Chinese Medical University, Hangzhou, Zhejiang, China

[5] Department of Orthopaedic Surgery, Fuyang Orthopaedics and Traumatology Affiliated Hospital of Zhejiang Chinese Medical University, Hangzhou, Zhejiang, China

[6] Research Center for Computer-aided Drug Discovery, Shenzhen Institute of Advanced Technology, Chinese Academy of Sciences, Shenzhen, 518005, China.

[7] Faculty of Pharmaceutical Sciences, Shenzhen Institute of Advanced Technology,

Chinese Academy of Sciences, Shenzhen, 518055, China.

[8] Department of Orthopaedic Surgery, the First Affiliated Hospital of Zhejiang Chinese Medical University，Zhejiang Provincial Hospital of Chinese Medicine, Hangzhou, Zhejiang, China

*** Corresponding authors:**

Hongting Jin, Institute of Orthopedics and Traumatology, The First Affiliated Hospital of Zhejiang Chinese Medical University, No.548, Binwen Road, Hangzhou, Zhejiang Province, 310053, China. Email: hongtingjin@163.com.

Peijian Tong, Institute of Orthopedics and Traumatology, The First Affiliated Hospital of Zhejiang Chinese Medical University, No.548, Binwen Road, Hangzhou, Zhejiang Province, 310053, China. Email: tongpeijian@163.com.

Di Chen, Faculty of Pharmaceutical Sciences, Shenzhen Institute of Advanced Technology, Chinese Academy of Sciences, No.1068, Xueyuan Avenue, Shenzhen, China. Email: di.chen@siat.ac.cn.

Conflicts of Interest

All authors declare that they have no conflict of interest.

Abstract

Backgroud: Recurrent joint bleeding in hemophilia patients frequently results in hemophilic arthropathy (HA). Drastic degradation of articular cartilage is a major characteristic of HA, but its pathological mechanisms has not yet been clarified. Here, we conducted a genome-wide DNA methylation study with the goal of identifying critical genes for HA cartilage degeneration.

Methods: DNA was isolated from human osteoarthritis (N = 5) and HA (N = 5) articular cartilages and analyzed using the Infinium Human Methylation 850 BeadChip array. Adeno-associated virus-mediated shRNA and siRNA were used to knock down Tenascin XB (TNXB) *in vivo* and *in vitro*, respectively. Then histopathological analysis, qPCR, Western blotting and immunofluorescence assays were conducted to detected chondrocyte homeostasis and HA progression.

Results: We found that DNMT1 and DNMT3A protein levels were increased in cartilages from HA patients compared with OA patients. Genome-wide DNA methylation analysis identified 1228 differentially methylated regions (DMRs) associated with HA. Functional enrichment analyses then revealed that DMR genes (DMGs) were related to extracellular matrix organization. Among these DMGs, TNXB protein expression was down-regulated in human and mouse HA cartilages. Further, the loss of *Tnxb* in $F8^{-/-}$ mouse cartilage provides a disease-promoting role in HA by augmenting cartilage matrix degeneration and subchondral bone loss. *Tnxb* knockdown also promoted chondrocyte apoptosis and inhibited phosphorylation of AKT. Importantly, AKT agonist showed a chondroprotective effect following *Tnxb*

knockdown.

Conclusions: our study demonstrated that TNXB is a central mediator of cartilage matrix degradation following joint bleeding, which functions by regulating the activation of AKT. These mechanistic insights allow targeted development of potentially new strategies for cartilage protection in HA.

Keywords: Hemophilic arthropathy; Methylation; Tenascin XB; Cartilage degeneration; Chondrocyte apoptosis.

Introduction

Hemophilia A and B are inherited bleeding disorders caused by a deficiency in coagulation factor VIII (FVIII) or factor IX (FIX), respectively. Joint bleeding (hemarthrosis) is the most common clinical manifestation in patients with severe hemophilia (i.e., plasma FVIII or FIX < 1 U/dl) [1]. Recent evidence also indicates that hemarthrosis may occur spontaneously in patients with moderate (plasma factor levels of 1– 5 UI/dl) or mild disease (plasma factor levels of >5 UI/dl) [2,3]. Repeated episodes of hemarthrosis eventually result in hemophilic arthropathy (HA), a debilitating and irreversible condition. HA often starts at an early age and characterized by joint impairment, chronic pain, and reduced quality of life [4-9].

Current efforts to prevent the development of HA are mainly focused on management of acute joint bleeding and optimizing prophylactic replacement therapy [1,10,11]. However, many hemophilia patients still experience the joint disease later in life, despite adequate prophylaxis, suggesting that pathological changes in soft tissue and bone, caused by breakthrough and/or sub-clinical bleeding of joint, accumulate over time, ultimately leading to joint deformities and HA [3,12]. Given no disease modifying therapy available to intervene in the HA perpetuating process, HA remains a persistent problem and challenge for hemophilia patients. Thus, to understand the pathogenesis of HA and subsequently explore possible targets for therapy is necessary.

One distinctive pathophysiological manifestation of HA is cartilage degeneration [13]. Cartilage is a rather inert tissue, consisting of matrix proteins and only one cell type,

chondrocytes that are responsible for production of matrix synthesis and rely on synovial fluid for nutrients as cartilage lacks blood supply [14,15]. Nevertheless, recurrent intra-articular bleeding creates a 'toxic' environment to cartilage, by inducing synovial inflammation, hemosiderin accumulation and excessive mechanical stress [13,16]. As a consequence, dysregulation of metabolism and abnormal apoptosis occur in chondrocytes, ultimately resulting in deterioration of the cartilage matrix [1].

DNA methylation, a core epigenetic mechanism, is high dynamic and susceptible to cues from the environment [17,18]. DNA methylation is the addition of a methyl group to the cytosine residue of DNA molecules, which is catalysed by DNA methyl transferase (DNMT) family of proteins that is comprised of three members: DNMT1, DNMT3a, and DNMT3b. DNA methylation is mainly located in the gene regulatory region, usually repressing gene expression by blocking the transcriptional accessibility of regulatory genomic regions [19]. Recently, multiple studies confirmed the important role of abnormal DNA methylation in the pathogenesis of arthritis [20,21]. However, the epigenetic mechanisms underlying HA-related cartilage degradation have not been explored.

In this study, we conducted a genome-wide DNA methylation study with the goal of identifying differentially methylated genes (DMGs) and pathways for HA. Further, we knocked down *Tnxb*, a key DMG, in primary mouse chondrocytes and hemophilia A ($F8^{-/-}$) mice. The biological function and underlying mechanisms of TNXB in HA progression were also investigated *in vivo* and *in vitro*. Our findings provide a new mechanism for articular cartilage lesion in HA, which may lead to the discovery of

novel therapeutic targets for the treatment of HA.

Materials and Methods

Cartilage specimen collection

In this study, 5 HA and 5 osteoarthritis knee cartilage specimens were collected from patients undergoing total knee replacement surgery. Knee cartilage tissues were dissected and then rapidly frozen in liquid nitrogen or fixed in 4% paraformaldehyde. All subjects were Chinese Han and their demographic characteristics were listed in Supplementary table 1. The human cartilage samples were obtained from Department of Orthopedic Surgery at The First Affiliated Hospital of Zhejiang Chinese Medical University. This study was approved by the Ethics Committee of the First Affiliated Hospital of Zhejiang Chinese Medical University (2019-ZX-004-02).

Genome-wide DNA methylation profiling

Genomic DNA was prepared from cartilage specimens using QIAamp DNA Blood Mini Kit (QIAGEN, Germany) according to the manufacturer’s instructions and was stored at -80 °C until used. Then bisulfite treatment of genomic DNA was performed with the EZ DNA methylation kit (Zymo Research) according to manufacturer's procedure. Genome-wide DNA methylation patterns were evaluated by Infinium Human Methylation 850 K BeadChips (Illumina), which determine the methylation levels of 853,307 CpG sites. R/Bioconductor (version 3.3.3) package ChAMP was used to process the Illumina intensity data (IDAT) files from the chip. DNA methylation level of each CpG site was described as a β value, ranging from zero (representing fully unmethylated) to one (representing fully methylated). Probes

that had a detection *P* value of > 0.01 and those located on the X and Y chromosome were filtered away. We also removed SNP-related probes and all multi-hit probes. BMIQ (Beta MIxture Quantile dilation) algorithm was used to correct for the Infinium type I and type II probe bias. Furthermore, the regression models were adjusted for age and sex. Differentially methylated probes (DMPs) at significance of $P < 0.05$ after the Benjamini & Hochberg correction for multiple testing. Differentially Methylated Regions (DMRs) were identified by Bumphunter with default settings. Additionally, we annotated the DMR-related genes (DMGs), and then performed Gene Ontology (GO) and Kyoto Encyclopedia of Genes (KEGG) pathway analysis by using the online tool DAVID (http://david.abcc.ncifcrf.gov/). The significant pathway/ GO term was identified with *P* value < 0.05.

Mouse

The FVIII target gene knockout hemophilia ($F8^{-/-}$) mouse were purchased from the Shanghai Laboratory Animal Center of the Chinese Academy of Sciences. All mouse were kept in the Laboratory Animal Center of Zhejiang University of Chinese Medicine. The animals were placed in the controlled environmental condition with relatively constant air humidity and temperature as well as manual control of day and night replacement for 12h. The experiment was approved by the Experimental Animal Ethics Committee of Zhejiang University of Traditional Chinese Medicine (LZ12H27001).

The mouse experimental model of HA

The HA model is constructed according to the description of Hakobyan et al [22].

$F8^{-/-}$ mouse were induced with 3% isoflurane, and 1% isoflurane was maintained under anesthesia. The right knee joint capsule of mouse was pierced with a 30g needle for bleeding modeling, and the left knee of each animal was used as a control group. Mouse were sacrificed at 4 and 8 weeks after injury, and knee joints were collected for further experiments.

Intra-articular injection

$F8^{-/-}$ mouse were induced with 3% isoflurane, and 1% isoflurane was maintained under anesthesia. The right knee joint capsule of mouse was pierced with a 30g needle for bleeding modeling. The needle of the insulin syringe was sagittally inserted into the intercondylar area of the mouse right knee joint, where 10 μl of AAV-Tnxb (GenePharma) or AAV-NC was injected. After 4 weeks, mouse was sacrificed, respectively, and the right knee joints were collected for further experiments.

Micro-computed tomography (μCT) analysis

Micro-computed tomography (μCT) (Skyscan 1176, Bruker μCT, Kontich, Gelgium) was used to analyze the knee joints. The area between the proximal tibia growth plate and the tibial plateau was chosen as the region of interest. The parameters collected form μCT were percent bone volume (BV/TV, %), Trabecular thickness (Tb.Th, mm), Trabecular number (Tb.N, 1/mm) and Trabecular Spacing(Tb.Sp, mm).

Histological analysis

The human cartilage samples were successively fixed in 4% paraformaldehyde for 5 days, decalcified with 14% EDTA solution for 3 months, and the mouse samples

were successively fixed in 4% paraformaldehyde for 3 days, decalcified with 14% EDTA solution for 14 days. These samples subsequently embedded in paraffin. Then 3-μm thick sections at the medial compartment of the joints were cut for Alcian blue hematoxylin/Orange G (ABH) or Toluidine Blue staining to analyze the gross cartilage structural changes. Histomorphometric analysis was performed through Osteomeasure software (Decatur, GA).

Immunohistochemistry

The immunohistochemistry was examined to observe the expressions of protein in cartilage. Briefly, the deparaffinized sections were soaked in 0.3% hydrogen peroxide to block the activity of endogenous peroxidase, then blocked with normal goat serum (diluted 1:20) for 20 min at room temperature. Subsequently, the primary antibodies were added and incubated overnight at 4° C. The next day, the sections were treated with secondary antibodies for 30 min and positive staining was visible by using diaminobenzidine solution (Invitrogen, MD, United States). Then counterstaining was performed with hematoxylin for 5 s. Anti-Col2a1 (Abcam, ab34712, 1:200), Anti-Mmp13 (Abcam, ab39012, 1:300), Anti-Tnxb (Proteintech, 13595-1-AP, 1:50), Anti-Bax (Huabio, ET1603-34, 1:200), Anti-Bcl-2 (Huabio, ET1702-53, 1:200), Anti-p-Akt1 (Abclonal, AP0140, 1:200), Dnmt1(Abcam, ab188453, 1：200), Dnmt3a (Abcam, ab2850, 1：200), Dnmt3b (Abcam, ab2851, 1：200) were used in this study.

Cell isolation and culture

Primary mouse chondrocytes were obtained from the femoral head of 2-week-old

C57BL/6J mouse purchased from the Experimental Animal Center of Zhejiang Chinese Medical University. Mouse were sacrificed and disinfected with 75% ethyl alcohol. Specimens were isolated and rinsed by Phosphate Buffer Saline (PBS) 3 times. Then the cartilage tissues were digested with 0.25% collagenase P at 37 °C for 4h. Chondrocytes were cultured in DMEM/F-12 medium containing 10% fetal bovine serum (FBS) and 1% streptomycin/penicillin in 5% CO_2 at 37 °C for further experiment.

Tunel assay.

To evaluate the apoptotic cells in the chondrocytes, we performed a Tunel assay according to the manufacturer's guideline (Beyotime, catalog C1088). Briefly, following deparaffinage and rehydration, sections were permeabilized with DNase-free Proteinase K (20 μg/mL) for 15 minutes at 37°C. Subsequently, slides were treated with Tunel solution and incubated at 37°C for 1 hour in a dark environment and counterstained with DAPI (1:1000; Solarbio) for 10 minutes. Finally, TUNEL positive cells were detected by fluorescence microscope.

Transfection of siRNA-*Tnxb*

Chondrocytes were transiently transfected with siRNA targeting *Tnxb* (GenePharma) or negative control siRNA (scrambled; GenePharma) using X tremeGENE siRNA transfection reagent (Sigma) following the manufacturer's instructions. All experiments were performed 72 hours after transfection, and the most effective single siRNA was used for further experiments. The effectiveness of transfection was determined by qPCR and western blotting assay. After transfection

for 48 h, cells were treated with SC79 (10μM, Selleck) for 24 h.

Cell Immunofluorescence

The cells were fixed with 4% paraformaldehyde and blocked with goat serum for 1 hour. Then, cells were incubated with Col2a1 antibody (1:200; Abcam) and Mmp13 antibody (1:100; Abcam) overnight. The next day, the knee joints samples and Chondrocytes with goat anti□rabbit antibody (1:1000; Invitrogen) conjugated with Alexa FluorTM 488 for 1 hour. Cells were stained with DAPI (1:1000; Solarbio).

Western blot analysis

Total proteins were extracted by RIPA buffer, and concentration of protein was determined by bicinchoninic acid (BCA, Beyotime, Shanghai, China). Proteins were separated on 10% SDS-PAGE gels and transferred to PVDF membranes. The membranes were then blocked with 5% skim milk for 1 h, and were incubated with primary antibodies (Col2a1, Abclonal, A1560, 1:1500), (Mmp13, Abclonal, A11755, 1:1000), (Tnxb, Abclonal, A2535, 1:1000), (p-Akt1, Abclonal, AP0140, 1:1000), (Akt1, Huabio, ET1609-47, 1:1000), (Bcl-2, Huabio, ET1702-53, 1:1000), (Bax, Huabio, ET1603-34, 1:1000), (active-pro caspase-3, Huabio, ET1608-64, 1:1000) overnight at 4°C. The membranes were washed 3 times, and then cultured with the secondary antibody for 1 h. The immunoreactivity was detected with the ECL substrate (Thermo Fisher Scientific, United States) on an Image Quant LAS 4000 (EG, United States). The grey value was calculated by the software of Image J. *β-actin* was used as an internal control in all western blot analysis.

Quantitative RT-PCR

TRIzol reagent (Invitrogen, United States) was used according to the manufacturer's protocol to extract total RNA from chondrocytes. The total RNA quantity and purity was evaluated by using NanoDrop 2000 (Thermo Fisher Scientific, United States). Reverse transcription was carried out with cDNA Synthesis Kit (Bmake, Beijing, China). The quantitative real-time-polymerase chain reaction (qRT-PCR) was conducted with SYBR Premix Ex Taq™ II (Takara, Dalian, China), and performed on on a QuantStudio™ 7 Flex Real□Time PCR System. All of the PCR reactions were repeated 3 times for each gene. The data were analyzed by the 2−ΔΔCT method using *β-actin* as the internal control. Supplementary table 2 showed the primer sequences of target genes used in the current study

Statistics

All experimental data of this subject were analyzed by GraphPad Prism software version 8.0, and the statistical results of measurement data were expressed as mean ± standard deviation. 2-tailed unpaired parametric Student's t test or nonparametric Mann-Whitney U test or one-way ANOVA with Tukey's multiple comparisons test was used for comparison between different groups. The difference was statistically significant with $P < 0.05$.

Results

Articular cartilages of HA patients show severe damage and aberrant elevations of DNMT1 and DNMT3A

In this study, we collected cartilage samples in tibial plateau from osteoarthritis and HA patients undergo total knee replacement (TKR) surgery. Consistent with

previous reports, the HA cartilage exhibited severe damage and significant hemosiderin deposition, compared with that of osteoarthritis (Figure 1A). MRI analysis revealed the subchondral bone loss in HA patients (Figure 1B). ABH staining further assessed the cartilage degeneration, and detected a substantial sulfated glycosaminoglycan (sGAG) depletion in HA cartilages (Figure 1, C and D). As expected, comparing to osteoarthritis, HA cartilages showed prominent decrease in cartilage matrix protein COL2A1 and increase in expression of MMP13, the primary enzymes responsible for cartilage degeneration (Figure 1, E and F). Additionally, obvious increase in DNMT1 and DNMT3A protein levels was also detected in HA cartilages (Figure 1, G and H), whereas no significant changes were found in DNMT3B (Supplemental Figure 1). These data confirmed the severe damage in articular cartilage and subchondral bone of HA patients.

Genome-wide DNA methylation analysis reveals the epigenetic landscape of HA cartilage

To understand the methylation profile associated with HA cartilage degeneration, genome-wide DNA methylation alterations were examined in 10 subjects (5 osteoarthritis cartilages and 5 HA cartilages) by using 850K ChIP. The methylation levels of whole genome-wide CpGs were in a classic bimodal distribution where most CpGs were either slightly or highly methylated (Figure 2A). Of note, global DNA methylation levels exhibited systematic differences between HA and osteoarthritis (OA), as illustrated by their separation pattern in principle component analysis (Figure 2B). Overall, 1228 significant differentially methylated regions (DMRs) ($P < 0.05$

after the Benjamini & Hochberg correction for multiple testing) were identified, with a mean fold change in methylation difference of 0.90 (Figure 2C, and Supplemental Table 3). Compared with the OA, 69.95% and 30.05% DMRs were hypermethylated and hypomethylated in HA, respectively (Supplemental Figure 2A). Given the specificity of DMR, we then determined whether the identified DMRs were preferentially colocalized with some specific genomic features. The large majority (93.49%) of these DMRs were located in gene promoters, 5'-UTRs, 3'-UTRs, and exons, with only 6.51% overlapping intergenic regions (Supplemental Figure 2B).

To determine the biological functions of these significant DMRs, GO and KEGG enrichment analysis were performed on DMR-related genes (DMGs). GO analysis revealed enrichment for terms largely related to extracellular matrix (ECM) organization, skeletal system development (Figure 2D, Supplementary Table 4). The top two KEGG pathways were ECM-receptor interaction (P value = 5.2×10^{-6}) and PI3K-Akt signaling pathway (P value = 5.3×10^{-4}) (Figure 2E, Supplementary Table 5). DMGs presented in these pathways have mostly been proved to play an important role in cartilage matrix homeostasis, such as *COL1A1*, *COL1A2*, *COMP* [23-25]. Among them, we found TNXB were significantly low expressed in human HA cartilage compared to OA cartilage by using IHC staining (Figure 1, F and G).

Decreased expression of Tnxb is associated with cartilage degradation by joint bleeding in $F8^{-/-}$ **mice**

To assess the potential relevance of TNXB in HA *in vivo*, we established a mouse model for HA, in which $F8^{-/-}$ mice received a needle puncture injury to the knee joint

[26,27]. This needle puncture induced excessive bleeding and caused severe hemarthrosis (Supplemental Figure 3A). Analysis of cartilage tissue sections by Toluidine blue staining uncovered that joint bleeding remarkably promoted cartilage degeneration at 4 and 8 weeks after injury (Figure 3, A and B). IHC staining further demonstrated lower expression of Col2a1 and increased expression of Mmp13 (Figure 3, C-F). Next, micro-CT was used to assess the influence of hemarthrosis in osteogenesis. An obvious osteopenia was detected in subchondral bone at 4 and 8 weeks post injury (Supplemental Figure 3, B-E). As expected, the above histopathological changes in $F8^{-/-}$ mice following needle puncture were similar with what we observed in Human HA. Meanwhile, decreased expression of Tnxb and increased expressions of Dnmt1 were showed in articular cartilages 4 and 8 weeks following injury (Figure 3, G-J). Above results suggest that TNXB might be protective against HA and its cartilage suppression is closely related to HA development.

***TNXB* knockdown impairs chondrocyte metabolism and aggravates the progression of HA**

To further identify the biological functions of TNXB in HA, we first knocked it down by specific siRNA in primary mouse chondrocytes. The efficiency of *Tnxb* knockdown was confirmed by results of qPCR and Western blot experiments (Figure 4, A-C). When compared with the siRNA-control group, we found that *Tnxb* knockdown led to a decrease in *Col2a1* mRNA expression and an increase in *Mmp13* mRNA expression (Figure 4D). Western blot and immunofluorescence staining analysis also showed a downregulated expression of Col2a1 protein and upregulated

expression of Mmp13 protein (Figure 4, E-H). Those observations revealed that TNXB positively regulated the metabolism of chondrocyte ECM.

Subsequently, we explored the effects of Tnxb on HA cartilage degradation *in vivo*, using intra-articular injection of adeno-associated virus (AAV) carrying *Tnxb*-specific short hairpin RNA (shRNA) in $F8^{-/-}$ mice. 4 weeks after injection, more severe cartilage degeneration was observed in *Tnxb*-KD mice, compared with vehicle group (Figure 4, I and J). In addition, *Tnxb*-KD mice showed decreased expression of Col2a1 and increased expression of Mmp13 in cartilages (Figure 4, K and L). The subchondral bone of *Tnxb*-KD mice was significantly less than vehicle group mice (Supplemental Figure 4, A-E). Collectively, the above results implied that TNXB knockdown in cartilage accelerated the HA development.

***TNXB* deficiency sensitizes chondrocytes to apoptosis by inhibiting AKT activation**

Since blood exposure in joint cavity strongly causes chondrocyte apoptosis (Supplemental Figure 5, A and B), we next explored the functional mechanisms of Tnxb in HA chondrocyte apoptosis. *Tnxb* knockdown induced the apoptosis in chondrocytes, as evidenced by an increased proportion of Tunel-positive cells (Figure 5, A and B). Meanwhile, protein expression levels of pro-apoptotic Bax and Cleaved-Caspase3 were significantly increased in *Tnxb*-KD chondrocytes, while anti-apoptotic Bcl-2 was decreased (Figure 5, C-F). Moreover, AAV-shTnxb injection also increased the number of Tunel-positive cells in articular cartilages in HA mice (Figure 5, G and H). IHC staining confirmed that Bcl-2 expression was significantly

reduced in *Tnxb*-KD HA mice accompanied by enhanced expressions of Bax and Caspase-3 (Figure 5, I-L).

It is well known that the PI3K/Akt signaling pathway regulates apoptosis [28-30], and our KEGG analysis and IHC staining confirmed the involvement of this pathway in HA cartilage degeneration (Figure 5, M and N). We, therefore, analyzed PI3K/Akt pathway following *Tnxb* knockdown. In *Tnxb*-KD chondrocytes, p-Akt protein level decreased significantly, while Akt level remained unchange (Figure 6, A and D). Next, we sought to investigate whether Akt activation could attenuate chondrocyte apoptosis induced by *Tnxb* knockdown. AKT agonist SC79 was used to treated *Tnxb*-KD chondrocytes, and then its efficiency was verified by western blotting (Supplemental Figure 5C). 24 hours after SC79 treatment, the expressions of Bcl-2 and Col2a1 (Figure 6, A, B and F) were upregulated, while Bax and Mmp13 expressions were markedly downregulated in *Tnxb*-KD chondrocytes (Figure 6, A, C and E). These findings indicate that *TNXB* knockdown induced chondrocyte apoptosis and ECM degradation through regulating AKT activation.

Discussion

HA, a common manifestation of hemophilia, is typical characterized by dramatic cartilage degradation [5]. Thus, the goal of our work was to provide a novel insight into pathogenic mechanisms underlying HA cartilage degeneration. Figure 6 G summarized our findings. Genome-wide DNA methylation analysis revealed the DNA methylation changes in cartilages from hemophilia patients and identified *TNXB* gene associated with HA. The decreased expression of TNXB protein was also confirmed

in both human and mouse HA cartilages. Further, *Tnxb* knockdown promoted ECM catabolism and chondrocyte apoptosis, and eventually accelerated the development of HA in $F8^{-/-}$ mice. Meanwhile, decreased TNXB expression inhibited the activation of Akt *in vivo* and *in vitro*. Notably, AKT agonist enhanced ECM synthesis and suppressed apoptosis in *Tnxb*-KD chondrocytes. From these findings, it could be hypothesized that abnormal methylation and decreased expression of TNXB are responsible for disruption of cartilage homeostasis in HA.

In hemophlia patients, recurrent joint bleeding creates a toxic environment including multifaceted processes such as hemosiderin deposition, inflammatory response and mechanical pressure overload [31-34]. DNA methylation is a dynamic epigenetic modification in response to environment. Using genome-wide DNA methylation analysis, we found 1228 significant DMRs associated with HA with 69.95% hypermethylated, which was also supported by a corresponding increase in DNMT1 and DNMT3A protein levels in HA cartilages. DNA methylation at gene promoter region is one of the important epigenetic mechanisms in the regulation of gene expression [35,36]. The identified HA-related DMRs showed high proportion in transcriptional start sites. These data suggest that DNA methylation is a critical mediator in the pathology of HA. Nevertheless, due to limited HA cartilage specimens, the mRNA transcription levels of DMR-related genes were not explored in this study. Further studies using additional HA samples will be conducted to investigate the possible transcriptional alteration of identified genes as well as their potential roles in HA development.

Furthermore, our enrichment analysis showed that DMR-related genes were significantly enriched in ECM organization and ECM-receptor interaction terms. It is consistent with previous reports that ECM acts as an epigenetic informational entity capable of transducing and integrating intracellular signals via ECM-receptor interaction [37-39]. DMR-related genes enriched in these terms, many are known to be critical compositions of cartilage matrix, such as *COMP*, *COL1A1* and *COL1A2* [23-25]. In Articular cartilage, ECM provides nutrients and mechanical support for chondrocytes [40], and its age-related stiffening epigenetically regulates gene expression and compromises chondrocyte integrity [41]. Above findings highlight that ECM-related genes are potential candidates for HA.

Tenascin-X (TNXB), an ECM glycoprotein, is the top differentially methylated gene in HA cartilages. Its expression was downregulated in human and mouse HA cartilages by IHC staining. TNXB belongs to tenascin family, whose members (TNC, TNR, TNXB, and TNW) share a similar domain pattern: an N-terminal oligomerization domain, a series of epidermal growth factor-like repeats, a variable number of fibronectin-type III (FNIII) repeats and a C-terminal fibrinogen-like domain [42]. Emerging evidence suggests the involvement of TNC in cartilage development and degeneration in arthritis [43,44]. Here, we prove for the first time a role of TNXB in cartilage homeostasis *in vivo* and *in vitro*. Specifically, *Tnxb* knockdown contributed to an increase in Mmp13 expression and decrease in Col2a1 expression in chondrocytes. In agreement with these findings, knockdown of *Tnxb* in cartilages of $F8^{-/-}$ mice resulted in accelerated HA-like lesions. The FNIII repeats domain of TNXB

undergoes alternative splicing to interact with different ECM proteins and growth factors, and then affects ECM network formation and three-dimensional collagen matrix stiffness [45]. Thus, future study would benefit from exploring the effect of the FNIII repeats domain in HA development to further clarify the specific mechanisms of TNXB.

The process of HA development is accompanied by the chondrocyte apoptosis which in part promotes the ECM degeneration [13,46]. We also observed remarkably increased apoptosis following joint bleeding in $F8^{-/-}$ mice. Interestingly, *Tnxb* knockdown could significantly induce apoptosis in chondrocytes *in vitro*, and even aggravate apoptosis in mouse HA cartilage, by enhancing expression of markers associated pro-apoptosis (Bax, C-Caspase3) and suppressing anti-apoptotic proteins (Bcl-2). In TNXB family, TNC was reported to inhibit human chondrosarcoma cell apoptosis by activation of Akt [47]. PI3K signaling pathway regulated Akt phosphorylation to suppress apoptosis [48,49]. Our KEGG ananlysis of DMGs showed the potential association of PI3K/Akt signaling with HA. We then detected much lower phosphorylation level of Akt in *Tnxb*-KD chondrocytes and HA models. In addition, AKT agonist effectively restored the abnormal Mmp13 expression and apoptosis induced by *Tnxb* knockdown. As evidenced by prior studies, AKT signaling can also affect cartilage metabolism by regulating Mmp13 expression [50,51]. These findings indicate that AKT activation mediates the effect of TNXB on HA chondrocytes apoptosis and ECM catabolism. Thus, therapeutic effect of AKT agonist on HA development deserves further study.

Conclusions

Conclusively, our study provides the first comprehensive methylation profile in the progression of knee HA, and shows that abnormal expression of TNXB is important in HA cartilage degeneration by suppressing the activation of AKT. These findings provide a new insight into mechanisms responsible for HA disease and suggest TNXB as a potentially novel therapeutic target for HA treatment.

List of abbreviations

HA: hemophilic arthropathy, DMRs: differentially methylated regions, DMGs: DMR genes, TNXB: Tenascin XB, DNMT: DNA methyl transferase, ABH: Alcian blue hematoxylin/Orange G, ECM: extracellular matrix, AAV: adeno-associated virus.

Study approval

In the current study, the human cartilage samples were obtained from Department of Orthopedic Surgery at The First Affiliated Hospital of Zhejiang Chinese Medical University. This study was approved by the Ethics Committee of the First Affiliated Hospital of Zhejiang Chinese Medical University (2019-ZX-004-02). And all the animal operating procedures in this study were approved by the Experimental Animal Ethics Committee of Zhejiang Chinese Medical University (LZ12H27001).

Data Availability Statement

The data used to provide support for the results of this study can be obtained from the corresponding authors.

Availability of data and materials

The datasets used and/or analysed during the current study are available from the corresponding author on reasonable request.

Conflicts of Interest

All authors declare that they have no conflict of interest.

Funding Statement

This research has been partially supported by the Natural Science Foundation of China (Grant nos. 82274280, 82104891, 82074457), the Natural Science Foundation of Zhejiang Province (LQ22H270006), the Fund for Distinguished Young Scholars of Zhejiang Province (LR23H270001).

Author contributions

J.C., Q.Z., D.C., P.T., and H.J. conceptualized the study. Q.Z. conducted the *in vivo* experiments. J.C., X.W. and R.X. collected the human samples and performed the *in vitro* assay. W.W., Y.H. and Q.S. analyzed the data. J.C. wrote the original draft and W.Y., P.W., D.C., P.T., and H.J. revised the manuscript critically for important intellectual content. D.C., P.T, and H.J. supervised this study. All the authors read and approved the final version of this manuscript.

Acknowledgments

We appreciate the great help from the Public Platform of Medical Research Center, Academy of Chinese Medical Science, Zhejiang Chinese Medical University.

Reference:

1. Gualtierotti, R., Solimeno, L.P., and Peyvandi, F. (2021). Hemophilic

arthropathy: Current knowledge and future perspectives. J Thromb Haemost *19*, 2112-2121. 10.1111/jth.15444.

2. Di Minno, M.N., Ambrosino, P., Franchini, M., Coppola, A., and Di Minno, G. (2013). Arthropathy in patients with moderate hemophilia a: a systematic review of the literature. Semin Thromb Hemost *39*, 723-731. 10.1055/s-0033-1354422.

3. Wyseure, T., Yang, T., Zhou, J.Y., Cooke, E.J., Wanko, B., Olmer, M., Agashe, R., Morodomi, Y., Behrendt, N., Lotz, M., et al. (2019). TAFI deficiency causes maladaptive vascular remodeling after hemophilic joint bleeding. JCI Insight *4*. 10.1172/jci.insight.128379.

4. Aledort, L.M., Haschmeyer, R.H., and Pettersson, H. (1994). A longitudinal study of orthopaedic outcomes for severe factor-VIII-deficient haemophiliacs. The Orthopaedic Outcome Study Group. J Intern Med *236*, 391-399. 10.1111/j.1365-2796.1994.tb00815.x.

5. Bolton-Maggs, P.H., and Pasi, K.J. (2003). Haemophilias A and B. Lancet *361*, 1801-1809. 10.1016/S0140-6736(03)13405-8.

6. Fischer, K., Bom, J.G., Mauser-Bunschoten, E.P., Roosendaal, G., and Berg, H.M. (2005). Effects of haemophilic arthropathy on health-related quality of life and socio-economic parameters. Haemophilia *11*, 43-48. 10.1111/j.1365-2516.2005.01065.x.

7. Manco-Johnson, M.J., Abshire, T.C., Shapiro, A.D., Riske, B., Hacker, M.R., Kilcoyne, R., Ingram, J.D., Manco-Johnson, M.L., Funk, S., Jacobson, L., et al.

(2007). Prophylaxis versus episodic treatment to prevent joint disease in boys with severe hemophilia. N Engl J Med *357*, 535-544. 10.1056/NEJMoa067659.

8. Oldenburg, J. (2015). Optimal treatment strategies for hemophilia: achievements and limitations of current prophylactic regimens. Blood *125*, 2038-2044. 10.1182/blood-2015-01-528414.

9. Olivieri, M., Kurnik, K., Pfluger, T., and Bidlingmaier, C. (2012). Identification and long-term observation of early joint damage by magnetic resonance imaging in clinically asymptomatic joints in patients with haemophilia A or B despite prophylaxis. Haemophilia *18*, 369-374. 10.1111/j.1365-2516.2011.02682.x.

10. Jackson, S.C., Yang, M., Minuk, L., Sholzberg, M., St-Louis, J., Iorio, A., Card, R., and Poon, M.C. (2015). Prophylaxis in older Canadian adults with hemophilia A: lessons and more questions. BMC Hematol *15*, 4. 10.1186/s12878-015-0022-8.

11. Schramm, W., Gringeri, A., Ljung, R., Berger, K., Crispin, A., Bullinger, M., Giangrande, P.L., Von Mackensen, S., Mantovani, L.G., Nemes, L., et al. (2012). Haemophilia care in Europe: the ESCHQoL study. Haemophilia *18*, 729-737. 10.1111/j.1365-2516.2012.02847.x.

12. Wojdasiewicz, P., Poniatowski, L.A., Nauman, P., Mandat, T., Paradowska-Gorycka, A., Romanowska-Prochnicka, K., Szukiewicz, D., Kotela, A., Kubaszewski, L., Kotela, I., et al. (2018). Cytokines in the

pathogenesis of hemophilic arthropathy. Cytokine Growth Factor Rev *39*, 71-91. 10.1016/j.cytogfr.2017.11.003.

13. Pulles, A.E., Mastbergen, S.C., Schutgens, R.E., Lafeber, F.P., and van Vulpen, L.F. (2017). Pathophysiology of hemophilic arthropathy and potential targets for therapy. Pharmacol Res *115*, 192-199. 10.1016/j.phrs.2016.11.032.

14. Fermor, B., Christensen, S.E., Youn, I., Cernanec, J.M., Davies, C.M., and Weinberg, J.B. (2007). Oxygen, nitric oxide and articular cartilage. Eur Cell Mater *13*, 56-65; discussion 65. 10.22203/ecm.v013a06.

15. Lafont, J.E. (2010). Lack of oxygen in articular cartilage: consequences for chondrocyte biology. Int J Exp Pathol *91*, 99-106. 10.1111/j.1365-2613.2010.00707.x.

16. van Vulpen, L.F.D., Holstein, K., and Martinoli, C. (2018). Joint disease in haemophilia: Pathophysiology, pain and imaging. Haemophilia *24 Suppl 6*, 44-49. 10.1111/hae.13449.

17. Feil, R., and Fraga, M.F. (2012). Epigenetics and the environment: emerging patterns and implications. Nat Rev Genet *13*, 97-109. 10.1038/nrg3142.

18. Jirtle, R.L., and Skinner, M.K. (2007). Environmental epigenomics and disease susceptibility. Nat Rev Genet *8*, 253-262. 10.1038/nrg2045.

19. Stelzer, Y., Shivalila, C.S., Soldner, F., Markoulaki, S., and Jaenisch, R. (2015). Tracing dynamic changes of DNA methylation at single-cell resolution. Cell *163*, 218-229. 10.1016/j.cell.2015.08.046.

20. Wang, W., Yu, Y., Hao, J., Wen, Y., Han, J., Hou, W., Liu, R., Zhao, B., He,

A., Li, P., et al. (2017). Genome-wide DNA methylation profiling of articular cartilage reveals significant epigenetic alterations in Kashin-Beck disease and osteoarthritis. Osteoarthritis Cartilage *25*, 2127-2133. 10.1016/j.joca.2017.08.002.

21. Zhang, Y., Fukui, N., Yahata, M., Katsuragawa, Y., Tashiro, T., Ikegawa, S., and Lee, M.T. (2016). Genome-wide DNA methylation profile implicates potential cartilage regeneration at the late stage of knee osteoarthritis. Osteoarthritis Cartilage *24*, 835-843. 10.1016/j.joca.2015.12.013.

22. Hakobyan, N., Enockson, C., Cole, A.A., Sumner, D.R., and Valentino, L.A. (2008). Experimental haemophilic arthropathy in a mouse model of a massive haemarthrosis: gross, radiological and histological changes. Haemophilia *14*, 804-809. 10.1111/j.1365-2516.2008.01689.x.

23. Chen, Y.R., Yang, K.C., Lu, D.H., Wu, W.T., Wang, C.C., and Tsai, M.H. (2019). The chondroprotective effect of diosmin on human articular chondrocytes under oxidative stress. Phytother Res *33*, 2378-2386. 10.1002/ptr.6425.

24. Maly, K., Andres Sastre, E., Farrell, E., Meurer, A., and Zaucke, F. (2021). COMP and TSP-4: Functional Roles in Articular Cartilage and Relevance in Osteoarthritis. Int J Mol Sci *22*. 10.3390/ijms22052242.

25. Zhang, H., Chen, C., Cui, Y., Li, Y., Wang, Z., Mao, X., Dou, P., Li, Y., and Ma, C. (2019). lnc-SAMD14-4 can regulate expression of the COL1A1 and COL1A2 in human chondrocytes. PeerJ *7*, e7491. 10.7717/peerj.7491.

26. Haxaire, C., Hakobyan, N., Pannellini, T., Carballo, C., McIlwain, D., Mak, T.W., Rodeo, S., Acharya, S., Li, D., Szymonifka, J., et al. (2018). Blood-induced bone loss in murine hemophilic arthropathy is prevented by blocking the iRhom2/ADAM17/TNF-alpha pathway. Blood *132*, 1064-1074. 10.1182/blood-2017-12-820571.

27. Magisetty, J., Kondreddy, V., Keshava, S., Das, K., Esmon, C.T., Pendurthi, U.R., and Rao, L.V.M. (2022). Selective inhibition of activated protein C anticoagulant activity protects against hemophilic arthropathy in mice. Blood *139*, 2830-2841. 10.1182/blood.2021013119.

28. Cai, C., Min, S., Yan, B., Liu, W., Yang, X., Li, L., Wang, T., and Jin, A. (2019). MiR-27a promotes the autophagy and apoptosis of IL-1beta treated-articular chondrocytes in osteoarthritis through PI3K/AKT/mTOR signaling. Aging (Albany NY) *11*, 6371-6384. 10.18632/aging.102194.

29. Hu, P.F., Chen, W.P., Bao, J.P., and Wu, L.D. (2018). Paeoniflorin inhibits IL-1beta-induced chondrocyte apoptosis by regulating the Bax/Bcl-2/caspase-3 signaling pathway. Mol Med Rep *17*, 6194-6200. 10.3892/mmr.2018.8631.

30. Luo, J., Manning, B.D., and Cantley, L.C. (2003). Targeting the PI3K-Akt pathway in human cancer: rationale and promise. Cancer Cell *4*, 257-262. 10.1016/s1535-6108(03)00248-4.

31. Hooiveld, M.J., Roosendaal, G., van den Berg, H.M., Bijlsma, J.W., and Lafeber, F.P. (2003). Haemoglobin-derived iron-dependent hydroxyl radical

formation in blood-induced joint damage: an in vitro study. Rheumatology (Oxford) *42*, 784-790. 10.1093/rheumatology/keg220.

32. Srivastava, A. (2015). Inflammation is key to hemophilic arthropathy. Blood *126*, 2175-2176. 10.1182/blood-2015-09-665091.

33. van Vulpen, L.F., van Meegeren, M.E., Roosendaal, G., Jansen, N.W., van Laar, J.M., Schutgens, R.E., Mastbergen, S.C., and Lafeber, F.P. (2015). Biochemical markers of joint tissue damage increase shortly after a joint bleed; an explorative human and canine in vivo study. Osteoarthritis Cartilage *23*, 63-69. 10.1016/j.joca.2014.09.008.

34. Visser, A.W., de Mutsert, R., le Cessie, S., den Heijer, M., Rosendaal, F.R., Kloppenburg, M., and Group, N.E.O.S. (2015). The relative contribution of mechanical stress and systemic processes in different types of osteoarthritis: the NEO study. Ann Rheum Dis *74*, 1842-1847. 10.1136/annrheumdis-2013-205012.

35. Kucuk, C., Hu, X., Jiang, B., Klinkebiel, D., Geng, H., Gong, Q., Bouska, A., Iqbal, J., Gaulard, P., McKeithan, T.W., and Chan, W.C. (2015). Global promoter methylation analysis reveals novel candidate tumor suppressor genes in natural killer cell lymphoma. Clin Cancer Res *21*, 1699-1711. 10.1158/1078-0432.CCR-14-1216.

36. Kulis, M., and Esteller, M. (2010). DNA methylation and cancer. Adv Genet *70*, 27-56. 10.1016/B978-0-12-380866-0.60002-2.

37. Jones, F.S., and Jones, P.L. (2000). The tenascin family of ECM glycoproteins:

structure, function, and regulation during embryonic development and tissue remodeling. Dev Dyn *218*, 235-259. 10.1002/(SICI)1097-0177(200006)218:2<235::AID-DVDY2>3.0.CO;2-G.

38. Kim, S.H., Turnbull, J., and Guimond, S. (2011). Extracellular matrix and cell signalling: the dynamic cooperation of integrin, proteoglycan and growth factor receptor. J Endocrinol *209*, 139-151. 10.1530/JOE-10-0377.

39. Alcaraz, L.B., Exposito, J.Y., Chuvin, N., Pommier, R.M., Cluzel, C., Martel, S., Sentis, S., Bartholin, L., Lethias, C., and Valcourt, U. (2014). Tenascin-X promotes epithelial-to-mesenchymal transition by activating latent TGF-beta. J Cell Biol *205*, 409-428. 10.1083/jcb.201308031.

40. Sutherland, A.J., Converse, G.L., Hopkins, R.A., and Detamore, M.S. (2015). The bioactivity of cartilage extracellular matrix in articular cartilage regeneration. Adv Healthc Mater *4*, 29-39. 10.1002/adhm.201400165.

41. Iijima, H., Gilmer, G., Wang, K., Bean, A.C., He, Y., Lin, H., Tang, W.Y., Lamont, D., Tai, C., Ito, A., et al. (2023). Age-related matrix stiffening epigenetically regulates alpha-Klotho expression and compromises chondrocyte integrity. Nat Commun *14*, 18. 10.1038/s41467-022-35359-2.

42. Tucker, R.P., Drabikowski, K., Hess, J.F., Ferralli, J., Chiquet-Ehrismann, R., and Adams, J.C. (2006). Phylogenetic analysis of the tenascin gene family: evidence of origin early in the chordate lineage. BMC Evol Biol *6*, 60. 10.1186/1471-2148-6-60.

43. Hasegawa, M., Yoshida, T., and Sudo, A. (2018). Role of tenascin-C in

articular cartilage. Mod Rheumatol *28*, 215-220. 10.1080/14397595.2017.1349560.

44. Hasegawa, M., Yoshida, T., and Sudo, A. (2020). Tenascin-C in Osteoarthritis and Rheumatoid Arthritis. Front Immunol *11*, 577015. 10.3389/fimmu.2020.577015.

45. Valcourt, U., Alcaraz, L.B., Exposito, J.Y., Lethias, C., and Bartholin, L. (2015). Tenascin-X: beyond the architectural function. Cell Adh Migr *9*, 154-165. 10.4161/19336918.2014.994893.

46. Hooiveld, M., Roosendaal, G., Wenting, M., van den Berg, M., Bijlsma, J., and Lafeber, F. (2003). Short-term exposure of cartilage to blood results in chondrocyte apoptosis. Am J Pathol *162*, 943-951. 10.1016/S0002-9440(10)63889-8.

47. Jang, J.H., and Chung, C.P. (2005). Tenascin-C promotes cell survival by activation of Akt in human chondrosarcoma cell. Cancer Lett *229*, 101-105. 10.1016/j.canlet.2004.12.012.

48. Tan, B.S., Tiong, K.H., Choo, H.L., Chung, F.F., Hii, L.W., Tan, S.H., Yap, I.K., Pani, S., Khor, N.T., Wong, S.F., et al. (2015). Mutant p53-R273H mediates cancer cell survival and anoikis resistance through AKT-dependent suppression of BCL2-modifying factor (BMF). Cell Death Dis *6*, e1826. 10.1038/cddis.2015.191.

49. Testa, J.R., and Bellacosa, A. (2001). AKT plays a central role in tumorigenesis. Proc Natl Acad Sci U S A *98*, 10983-10985.

10.1073/pnas.211430998.

50. El Mabrouk, M., Sylvester, J., and Zafarullah, M. (2007). Signaling pathways implicated in oncostatin M-induced aggrecanase-1 and matrix metalloproteinase-13 expression in human articular chondrocytes. Biochim Biophys Acta *1773*, 309-320. 10.1016/j.bbamcr.2006.11.018.

51. Lu, J., Feng, X., Zhang, H., Wei, Y., Yang, Y., Tian, Y., and Bai, L. (2021). Maresin-1 suppresses IL-1beta-induced MMP-13 secretion by activating the PI3K/AKT pathway and inhibiting the NF-kappaB pathway in synovioblasts of an osteoarthritis rat model with treadmill exercise. Connect Tissue Res *62*, 508-518. 10.1080/03008207.2020.1780218.

Figure 1. The severe cartilage damage in human HA. (A) Human cartilage samples in the tibial plateau were obtained from patients with OA and HA. **(B)** MRI imaging of the knee joint in patients with HA and OA. Red arrow indicates the wear area. **(C)** Representative images of ABH/OG staining for HA and OA cartilage. **(D)** The degree of cartilage degeneration was quantified according to the OARSI score. **(E)** Representative IHC staining of COL2A1 and MMP13. **(F)** Quantification of the proportion of COL2A1 and MMP13 positive regions in human cartilage. **(G)** Representative IHC staining of DNMT1 and DMMT3A. **(H)** Quantification of the proportion of NMT1 and DMMT3A positive cells in human cartilage. Red arrows

indicate positive cells. Scale bar: 100 μm. Data were presented as means ± SD and analyzed by 2-tailed unpaired parametric Student's t test, $^{**}P < 0.01$, $^{***}P < 0.001$.

Figure 2. Genome-wide DNA methylation profile in HA cartilage and biological functions of DMR-Related genes. (A) Distribution of methylation level density of CpGs. Note: X = degree of methylation; Y = the CpG site density corresponding to the level of methylation. **(B)** Principle component analysis of DNA methylation data. **(C)** Heatmap shows the 700 signifricant DMRs between HA and OA. **(D)** Enriched GO terms for DMR-related genes. **(E)** KEGG enrichment analysis of DMR-related genes. **(F)** Representative IHC staining of TNXB. Red arrows indicate positive areas. Scale bar: 100 μm. **(G)** Quantification of the proportion of TNXB positive regions in human cartilage. Data were presented as means ± SD and analyzed by 2-tailed unpaired parametric Student's t test, $^{***}P < 0.001$.

Figure 3. TNXB expression is drastically reduced in HA mouse cartilages. (A) Representative images and **(B)** Quantitative analysis of Toluidine blue staining for knee sections of $F8^{-/-}$ mice at 4 and 8 weeks following injury. Representative IHC staining of **(C)** Col2a1, **(E)** Mmp13, **(G)** Tnxb, and **(I)** Dnmt1 in $F8^{-/-}$ mice at 4 and 8 weeks post injury. Quantification of the proportion of **(D)** Col2a1, **(F)** Mmp13, **(H)** Tnxb and (**J)** Dnmt1 positive regions. Scale bar: 100 μm. Data were presented as means ± SD and analyzed by 2-tailed unpaired parametric Student's t test, $^{***}P < 0.001$, $n \geq 3$ in each group.

Figure 4. knockdown of Tnxb in chondrocytes induces extracellular matrix degradation and accelerates the progression of HA. (A) qPCR and **(B)** Western blotting analysis for Tnxb in mouse chondrocytes treated with siRNA-NC or siRNA-*Tnxb*. **(C)** Corresponding quantification analysis of Tnxb protein. Quantification of mRNA levels for **(D)** *Mmp13* and*Col2a1* in *Tnxb*-KD chondrocytes. **(E)** Western blot and **(F)** corresponding quantification analysis forMmp13 and Col2a1 protein. **(G)** Representative immunofluorescence images of Col2a1 and Mmp13 expression in *Tnxb*-KD chondrocytes. **(H)** Quantification of Col2a1 and Mmp13 fluorescence intensity. Representative images of **(I)** Toluidine blue staining and **(K)** IHC staining of Mmp13 and Col2a1 for knee sections of $F8^{-/-}$ mice at 4 weeks after Intra-articular injection of AAV-sh*Tnxb*. **(J)** Quantitative detection of the area of the tibial cartilage area. **(L)** Quantification of the proportion of Col2a1 and Mmp13 positive regions.Red arrow indicates the wear area. Scale bar: 100 μm. Data were presented as means ± SD and analyzed by 2-tailed unpaired parametric Student's t test, $*P < 0.05$, $**P < 0.01$, $***P < 0.001$, $n \geq 3$ in each group.

Figure 5. Tnxb knockdown increases apoptosis in chondrocytes and HA cartilages. (A) Representative images of TUNEL staining in Tnxb-KD chondrocytes **(B)** Quantification for TUNEL positive cells. **(C-F)** Western blot and corresponding quantification analysis for Bax, Cleaved-Caspase3, and Bcl-2. **(G)** TUNEL staining for apoptosis in articular cartilage from Tnxb-KD HA mice. **(H)** Quantification for

TUNEL positive cells in articular cartilage. Representative IHC staining of Bax **(I)**, Bcl-2 **(K)**, and p-Akt1 **(M)** in articular cartilage from *Tnxb*-KD HA mice. Corresponding quantification of the proportion of **(J)** Bax, **(L)** Bcl-2 and **(N)** p-Akt1 positive regions. Red arrows indicate positive cells. Scale bar: 100 μm. Data were presented as means ± SD and analyzed by 2-tailed unpaired parametric Student's t test, $^{**}P < 0.01$, $^{***}P < 0.001$, $n \geq 3$ in each group.

Figure 6. Treatment with AKT agonist decreases apoptosis in TNXB-KD chondrocytes. (A) Western blot analysis for Col2a1, Mmp13, Bax, Bcl-2, p-Akt1 and Akt1 in Tnxb-KD chondrocytes treated with SC79 (0 or 10μM) for 24 hours. **(B-F)** Corresponding quantification of these proteins. **(G)** Schematic of the role of TNXB in the pathogenesis of HA cartilage degeneration. Data were presented as means ± SD and analyzed by 2-tailed unpaired parametric Student's t test or one-way ANOVA with Tukey's multiple comparisons test, $^{*}P < 0.05$, $^{**}P < 0.01$, $^{***}P < 0.001$, $n \geq 3$ in each group.

Figure 1

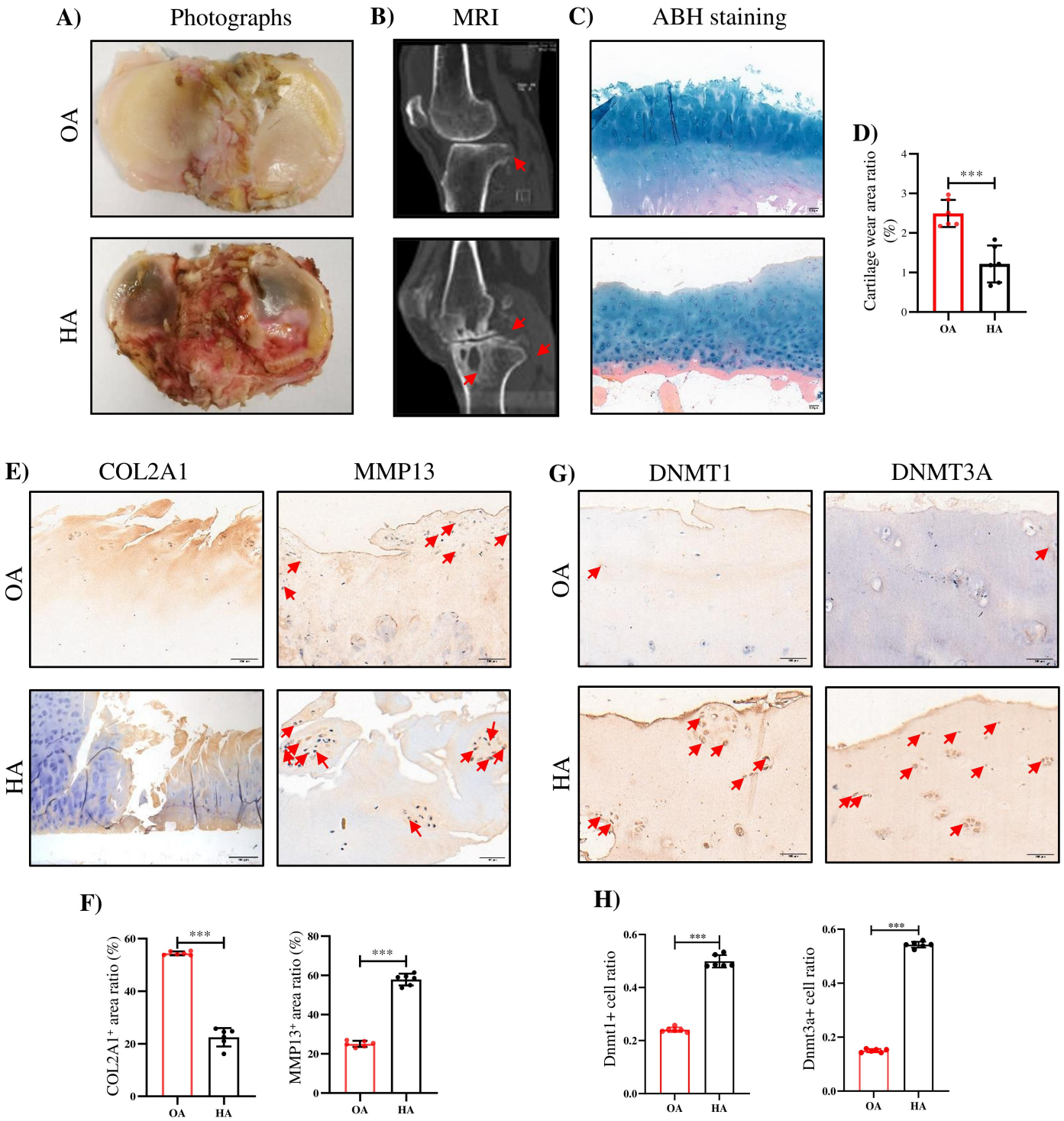
A)
Photographs
B)
MRI
C)
ABH staining
OA
HA
D)
Cartilage wear area ratio (%)
***
OA
HA
E)
COL2A1
MMP13
OA
HA
G)
DNMT1
DNMT3A
OA
HA
F)
COL2A1+ area ratio (%)
MMP13+ area ratio (%)
***
OA
HA
H)
Dnmt1+ cell ratio
Dnmt3a+ cell ratio
***
OA
HA

Figure 2

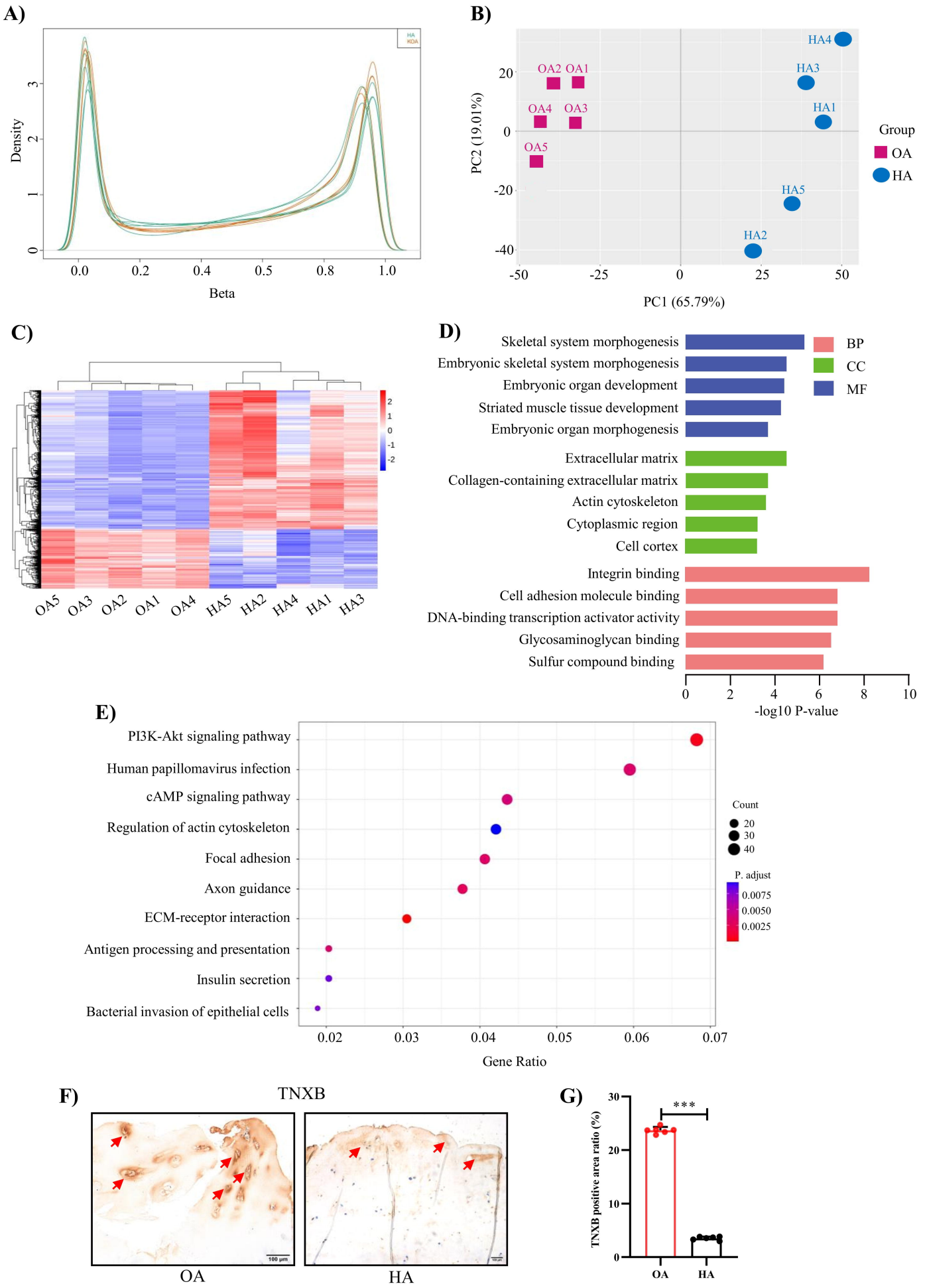
A)
HA
KOA
Density
Beta
0.0
0.2
0.4
0.5
0.8
1.0
B)
OA2
OA1
OA4
OA3
OA5
HA4
HA3
HA1
HA5
HA2
PC2 (19.01%)
PC1 (65.79%)
Group
OA
HA
C)
OA5
OA3
OA2
OA1
OA4
HA5
HA2
HA4
HA1
HA3
D)
Skeletal system morphogenesis
Embryonic skeletal system morphogenesis
Embryonic organ development
Striated muscle tissue development
Embryonic organ morphogenesis
Extracellular matrix
Collagen-containing extracellular matrix
Actin cytoskeleton
Cytoplasmic region
Cell cortex
Integrin binding
Cell adhesion molecule binding
DNA-binding transcription activator activity
Glycosaminoglycan binding
Sulfur compound binding
BP
CC
MF
-log10 P-value
E)
PI3K-Akt signaling pathway
Human papillomavirus infection
cAMP signaling pathway
Regulation of actin cytoskeleton
Focal adhesion
Axon guidance
ECM-receptor interaction
Antigen processing and presentation
Insulin secretion
Bacterial invasion of epithelial cells
Gene Ratio
Count
P. adjust
F)
TNXB
OA
HA
G)
TNXB positive area ratio (%)
***
OA
HA

Figure 3

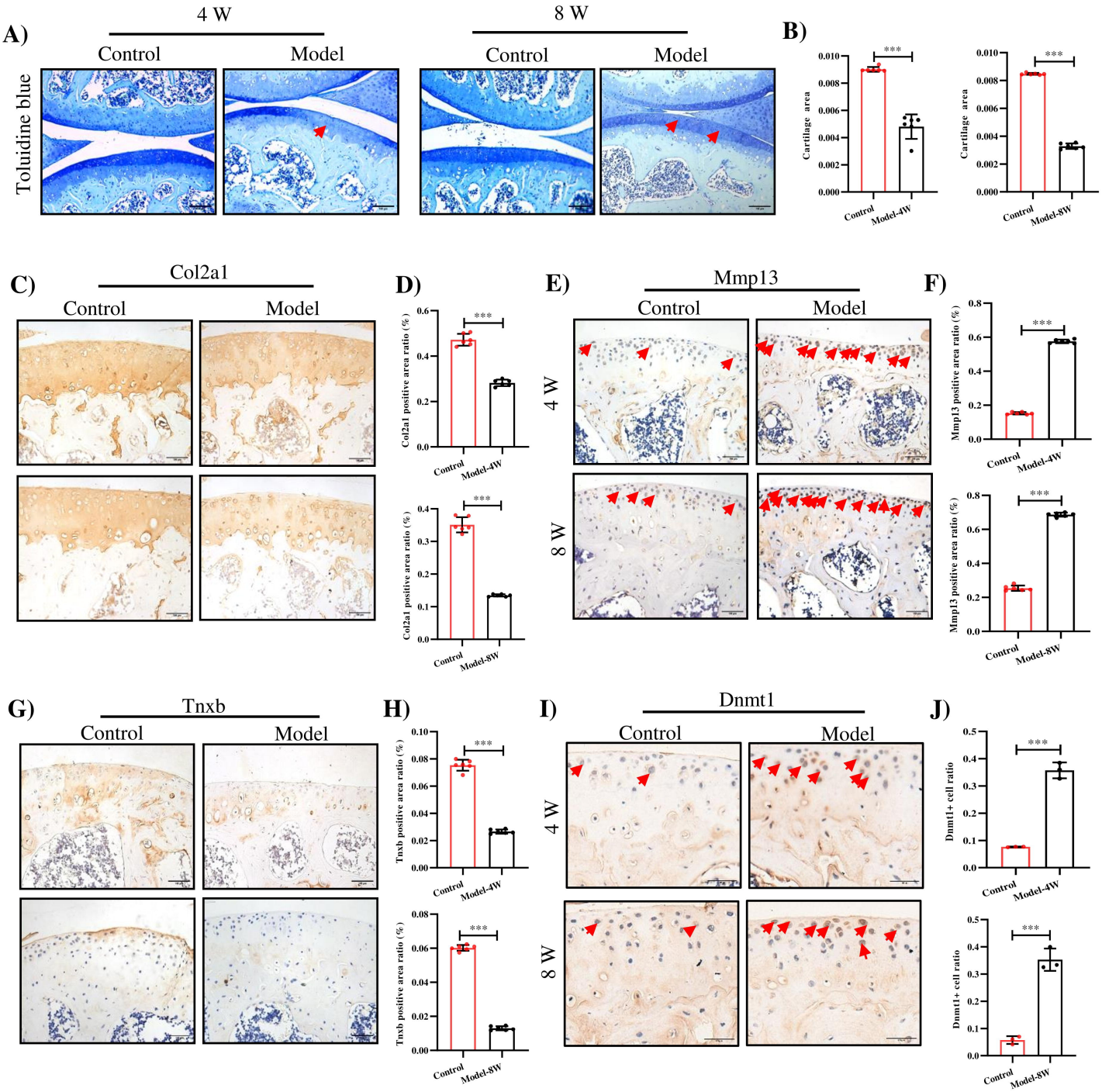
A)
4 W
8 W
Control
Model
Control
Model
Toluidine blue
B)
Cartilage area
Control
Model-4W
Model-8W
C)
Col2a1
Control
Model
D)
Col2a1 positive area ratio (%)
E)
Mmp13
4 W
8 W
F)
Mmp13 positive area ratio (%)
G)
Tnxb
H)
Tnxb positive area ratio (%)
I)
Dnmt1
J)
Dnmt1+ cell ratio
***

Figure 4

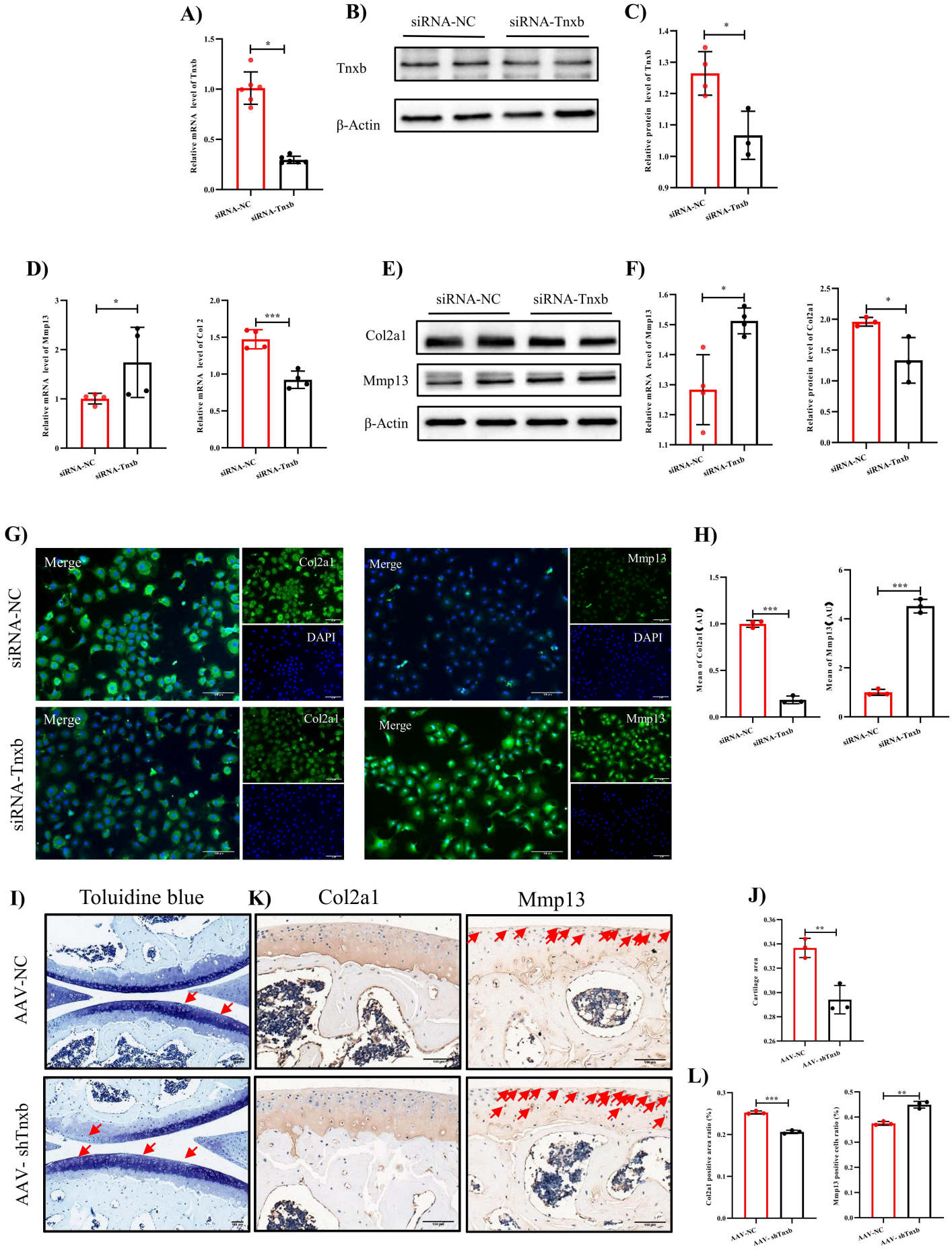
A)
Relative mRNA level of Tnxb
siRNA-NC
siRNA-Tnxb
B)
siRNA-NC
siRNA-Tnxb
Tnxb
β-Actin
C)
Relative protein level of Tnxb
D)
Relative mRNA level of Mmp13
Relative mRNA level of Col 2
E)
Col2a1
Mmp13
F)
Relative protein level of Col2a1
G)
Merge
Col2a1
DAPI
Mmp13
H)
Mean of Col2a1（AU）
Mean of Mmp13（AU）
I)
Toluidine blue
K)
Col2a1
Mmp13
AAV-NC
AAV- shTnxb
J)
Cartilage area
L)
Col2a1 positive area ratio (%)
Mmp13 positive cells ratio (%)

Figure 5

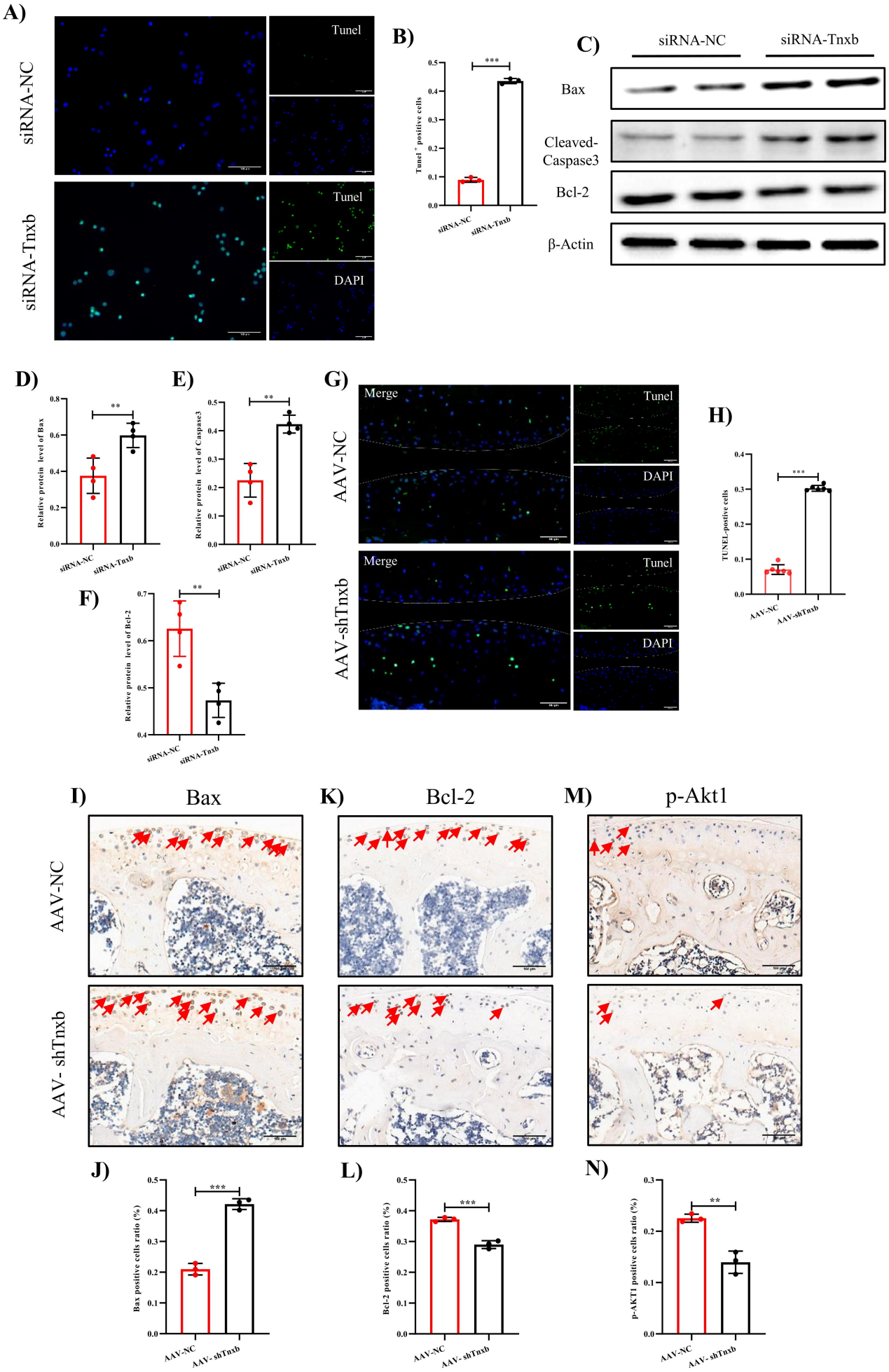
A)
siRNA-NC
siRNA-Tnxb
Tunel
DAPI
B)
Tunel + positive cells
siRNA-NC
siRNA-Tnxb
C)
siRNA-NC
siRNA-Tnxb
Bax
Cleaved-Caspase3
Bcl-2
β-Actin
D)
Relative protein level of Bax
E)
Relative protein level of Caspase3
F)
Relative protein level of Bcl-2
G)
AAV-NC
AAV-shTnxb
Merge
Tunel
DAPI
H)
TUNEL-postive cells
I)
Bax
K)
Bcl-2
M)
p-Akt1
AAV-NC
AAV- shTnxb
J)
Bax positive cells ratio (%)
L)
Bcl-2 positive cells ratio (%)
N)
p-AKT1 positive cells ratio (%)

Figure 6

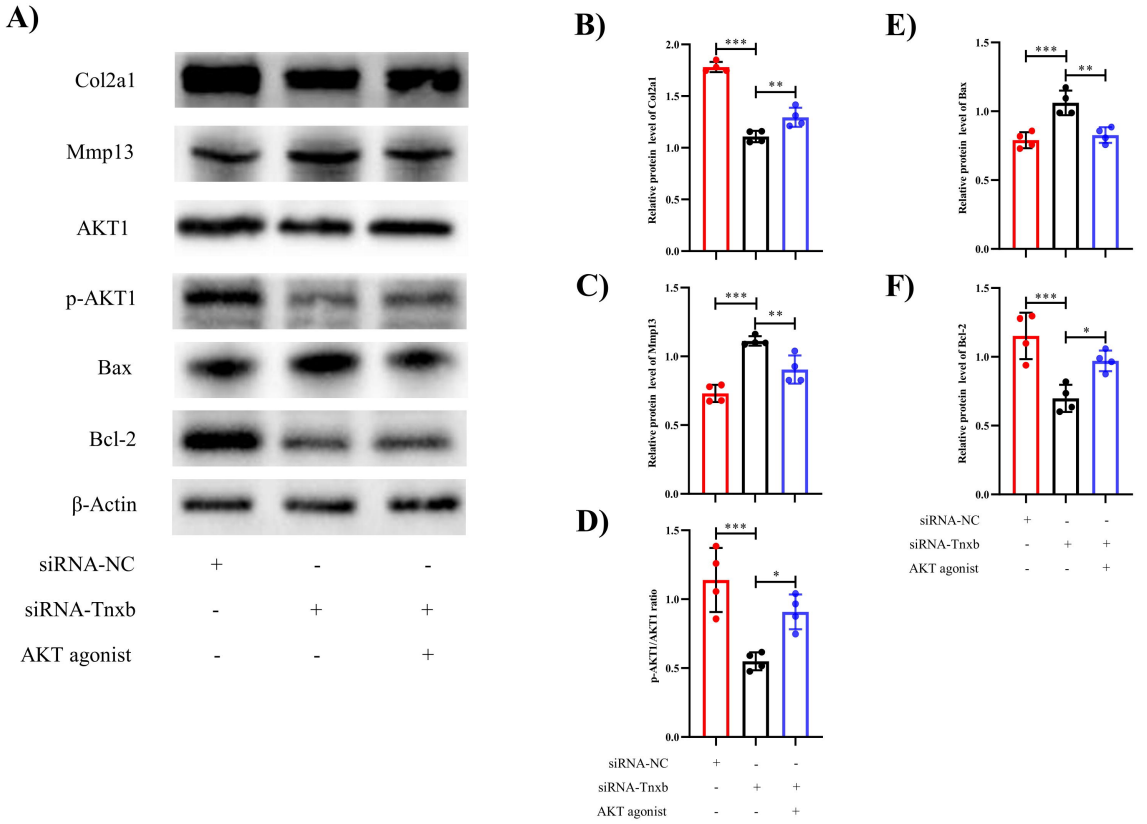
A)
Col2a1
Mmp13
AKT1
p-AKT1
Bax
Bcl-2
β-Actin
siRNA-NC + - -
siRNA-Tnxb - + +
AKT agonist - - +
B)
Relative protein level of Col2a1
C)
Relative protein level of Mmp13
D)
p-AKT1/AKT1 ratio
E)
Relative protein level of Bax
F)
Relative protein level of Bcl-2
siRNA-NC + - -
siRNA-Tnxb - + +
AKT agonist - - +

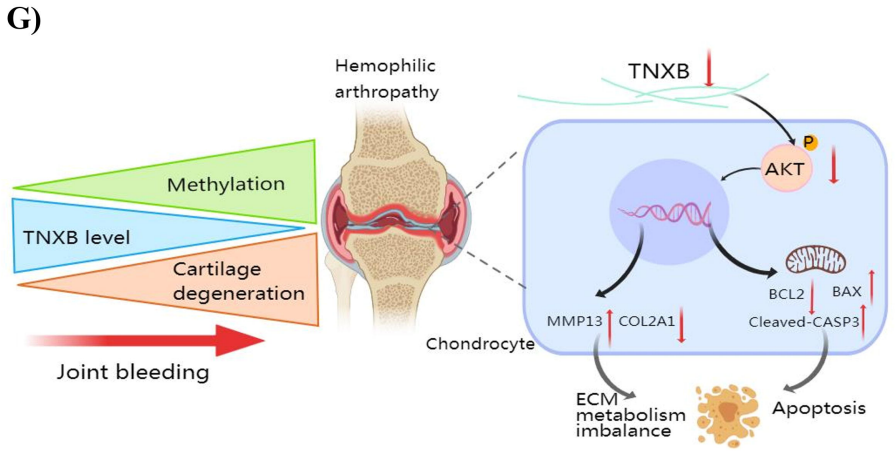
G)
Hemophilic arthropathy
Methylation
TNXB level
Cartilage degeneration
Joint bleeding
TNXB
AKT
P
BCL2
BAX
MMP13
COL2A1
Cleaved-CASP3
Chondrocyte
ECM metabolism imbalance
Apoptosis